

Supramolecular Polymer of Near-Infrared Luminescent Porphyrin Glass

Mitsuhiko Morisue,^{*,a} Yuki Hoshino,^a Masaki Shimizu,^a Takayuki Nakanishi,^b Yasuchika Hasegawa,^b Md. Amran Hossain,^c Shinichi Sakurai,^c Sono Sasaki,^c Shinobu Uemura,^d and Jun Matsui^e

^aFaculty of Molecular Chemistry and Engineering and ^c Faculty of Fiber Science and Engineering, Kyoto Institute of Technology, Matsugasaki, Sakyo-ku, Kyoto 606-8585, Japan.

^bGraduate School of Engineering, Hokkaido University, North 13 West 8, Kita-ku, Sapporo 060-8628, Japan.

^dDepartment of Advanced Materials Science, Kagawa University, Hayashi-cho, Takamatsu 761-0396, Japan.

^eDepartment of Material and Biological Chemistry, Faculty of Science, Yamagata University, Kojirakawa-cho, Yamagata, 990-8560, Japan.

Contents

1. Supramolecular Polymerisation in Toluene	S1
2. AFM observation	S3
3. Photophysical Measurements	S3
4. GISAXS	S3

1. Supramolecular Polymerization in Toluene

In the ¹H NMR spectrum of **1** in toluene-*d*₈ as a non-coordinating solvent, the protons of the pyridyl group emerged in a non-aromatic region, which suggested an

upfield shift due to strong shielding in the vicinity of the porphyrin plane (Figure S1A) and that two equivalent porphyrin planes were slipped-cofacially stacked through self-complementary coordination bonds. For instance, in pyridine-*d*₅ as a competitively coordinating solvent, the emergence of the non-shielded pyridyl protons was observed instead of the disappearance of the resonances in non-aromatic region (Figure S1B). Based on the binding constant estimated spectral change, as described in the main text, **1** was assumed to produce an oligomeric array (~50-mer) at 12 mM in toluene. No

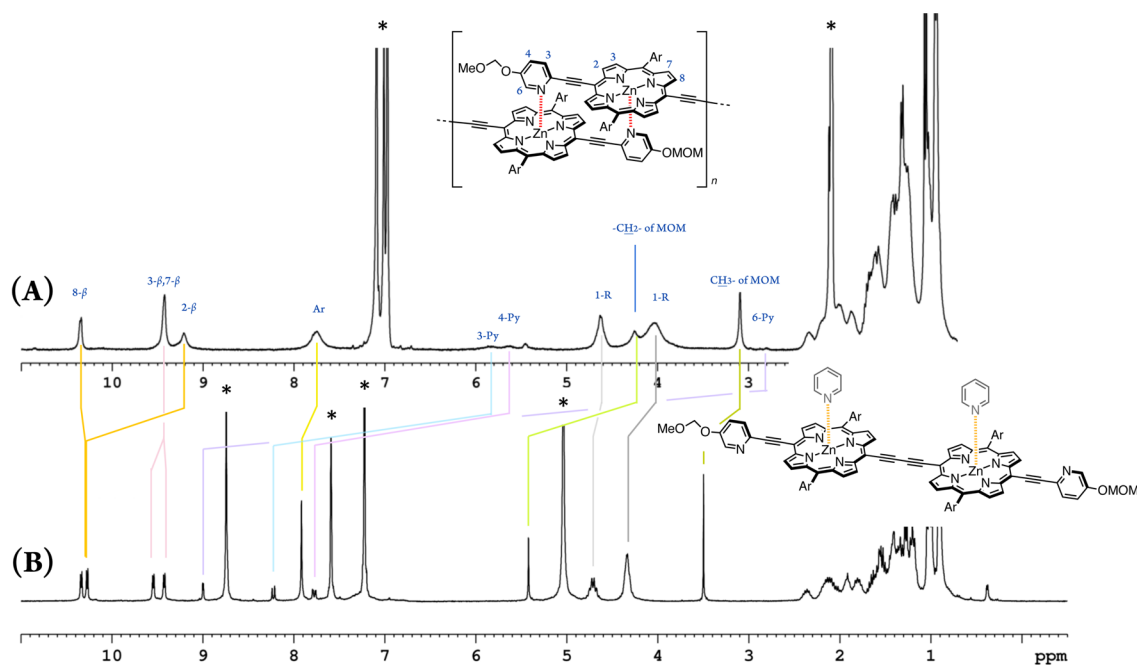


Figure S1. ¹H NMR spectra of 12 mM of **1** in toluene-*d*₈ (A) and in pyridine-*d*₅ (B) (300 MHz, 25 °C).

signals of the terminal units were observed owing to rapid averaging of the environments of all the protons on the NMR time scale.

The 2D NMR spectra, totally correlated spectroscopy (TOCSY) and nuclear Overhauser effect spectroscopy (NOESY) supported the formation of supramolecular polymer (Figure S2). Unambiguous NOE correlation

between the methyl proton of the MOM terminal and the β -protons of the porphyrin ring elucidated the cofacially stacked conformation in the supramolecular polymer of **1**.

The binding constant was estimated from the spectral change based on the following equation.^{S1}

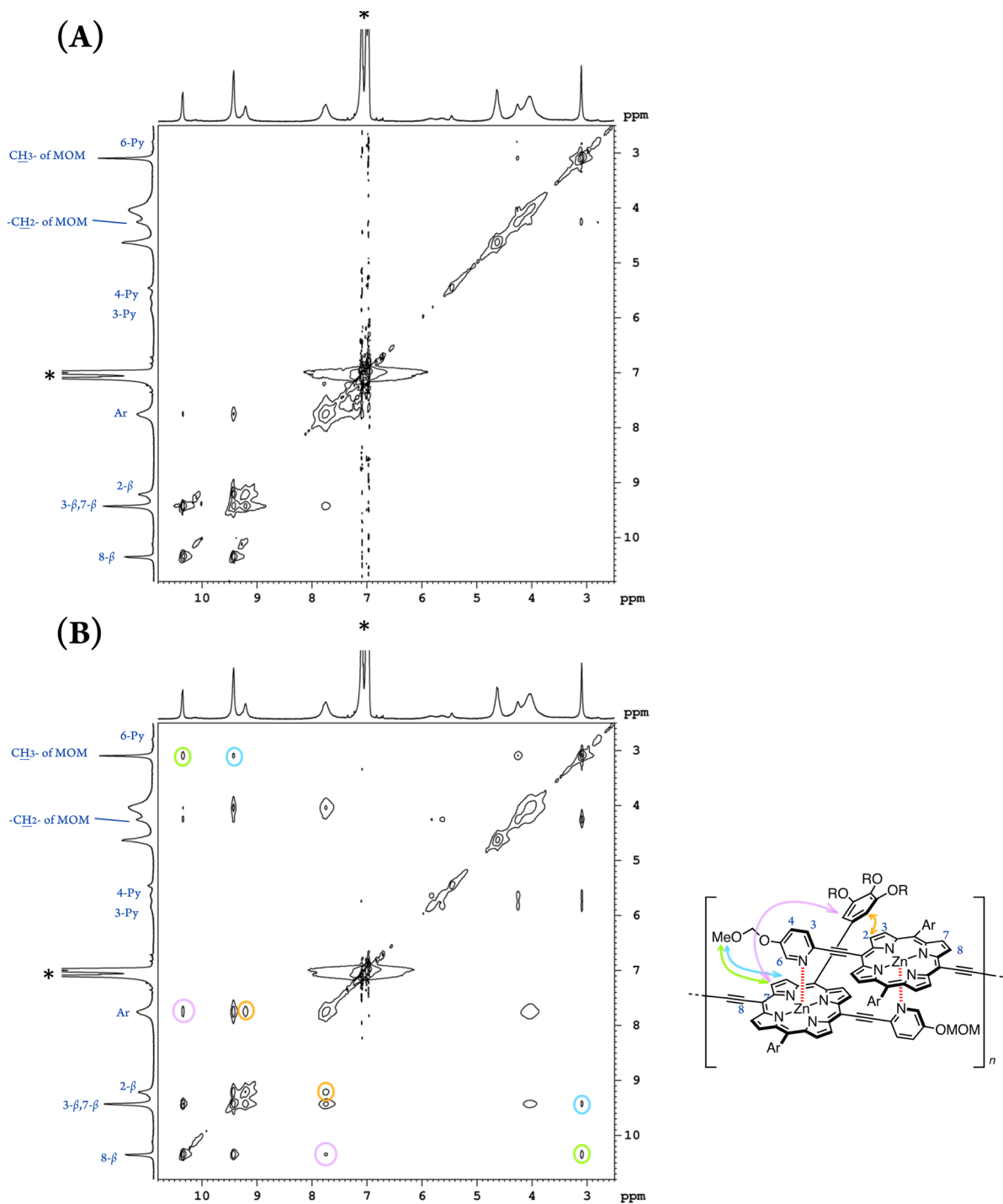


Figure S2. ^1H - ^1H TOCSY (A) and NOESY (B) spectra of **1** in toluene- d_8 (300 MHz, 25 °C). The asterisk indicates residual solvent.

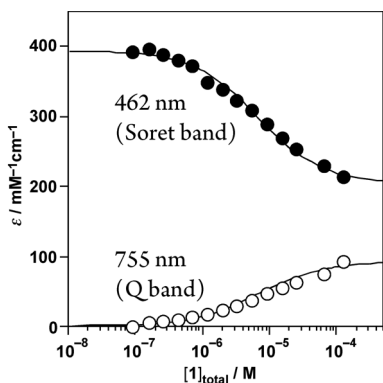


Figure S3. Plots of spectral variation at 462 (filled circles) and 755 nm (open circles), and the simulated curve assuming $K \approx 9 \times 10^4$ M^{-1} in the isodesmic supramolecular polymerisation model.

$$\varepsilon = \frac{2K[1]_{\text{total}} + 1 - \sqrt{1 + 4K[1]_{\text{total}}}}{2K^2[1]_{\text{total}}^2} (\varepsilon_{\text{mono}} - \varepsilon_{\text{poly}}) + \varepsilon_{\text{poly}} \quad (\text{S1})$$

wherein $\varepsilon_{\text{mono}}$ and $\varepsilon_{\text{poly}}$ are the extinction coefficient of the monomeric and polymeric species, respectively, and $[1]_{\text{total}}$ is total concentration of **1**. According to this formulation, the binding constant of **1** was estimated from spectrometric change (FIGURE 1A in the main text) to be approximately 9.0×10^4 M^{-1} (Figure S3).

The weight-average degree of polymerization ($\langle dp \rangle_w$) is here employed as the number of repeat units. The $\langle dp \rangle_w$ value for isodesmic model is formulated as follows:

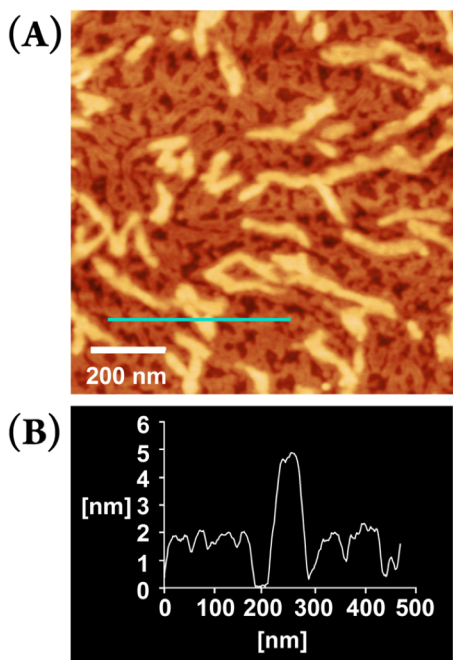


Figure S4. AFM image of the part of the spin-cast film of **1** with monomolecular thickness together with partially double-layered thickness (the bright parts) (A), cross-section along the blue line (B).

$$n \approx \langle dp \rangle_w = (1 + K[1]) / (1 - K[1]) \quad (\text{S2})$$

wherein $K[1]$ is defined as

$$K[1] = 1 + \frac{1}{2K[1]_{\text{total}}} - \sqrt{\frac{1}{K[1]_{\text{total}}} + \frac{1}{4K^2[1]_{\text{total}}^2}} \quad (\text{S3})$$

Polydispersity, PDI, is described as

$$\text{PDI} = 1 + K[1] \quad (\text{S4})$$

According to the above equations, **1** was estimated to produce a \sim heptamer with broad polydispersity (~ 1.7) at 10^{-4} M in toluene.

2. AFM Observation

A typical AFM image of a thinner part of the spin-cast film (Figure S4) revealed that fibrillar structures with uniform width on the whole surface, and the second fibrillar layers in part (the bright domains on Figure S4). The difference in height between the first and the second layers was 2.8 ± 0.3 nm.

3. Photophysical Measurements

In THF solution, the fluorescence lifetime of monomeric **1** was too short to determine a reliable decay time constant under our experimental conditions, but it was at least shorter than 1 ns. Figure S5 represents the emission decay profiles at 800 and 1025 nm.

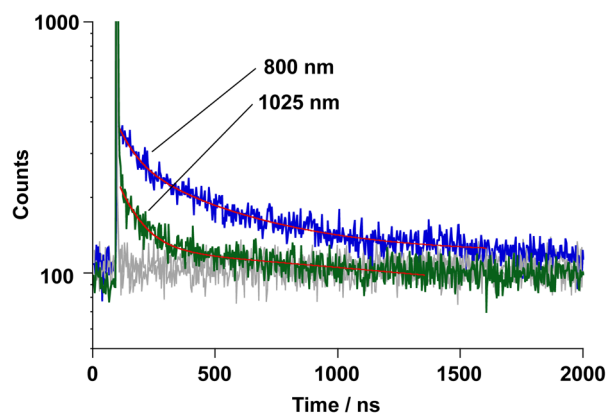


Figure S5. Emission decay profile of supramolecular array of **1** in the spin-cast film monitored at 800 nm (blue line) and at 1025 nm (green line), where the fitting curve and instrumental response function is shown in red and gray, respectively.

4. Synchrotron Glazing-incidence Small Angle X-ray Scattering (GISAXS):

In Figure S6, GISAXS caused by the transmitted and reflected X-rays was detected at the same time. By changing the incident angle from 0 to 0.15 deg., GISAXS caused by the reflected X-rays decreased in intensity, as the total reflection of the incident X-rays did not occur at the sample or substrate surface (Figure S6 and S7, also see Figure 3 in the main text).

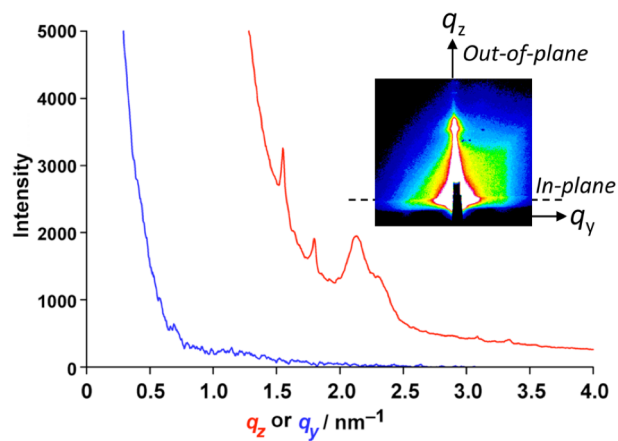


Figure S6. Out-of-plane and in-plane GISAXS profiles measured for the supramolecular multiporphyrin array prepared on a hydrophobised silicon wafer. The inserted image shows a GISAXS pattern measured at an incident angle of the direct beam of 0.12° .

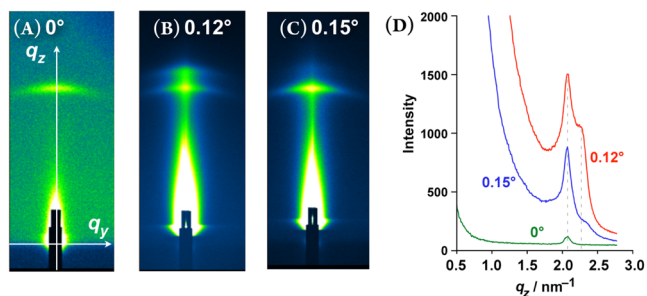


Figure S7. GISAXS patterns of the supramolecular multiporphyrin array measured at incident angles of the direct X-rays of 0° (A), 0.12° (B) and 0.15° (C) and their out-of-plane intensity profiles averaged over an azimuthal region of ± 2 deg. from the q_z axis (D). The peaks at q_z of ca. 2.0 and 2.3 were reflections from the same sample in transmission and reflection geometries in GISAXS, respectively.

REFERENCES

- S1 Haino, T.; Fujii, T.; Watanabe, A.; Takayanagi, U. *Proc. Natl. Acad. Sci. USA* **2009**, *26*, 10477–10481.
 S2 Zhao, D.; Moore, J. S. *Org. Biomol. Chem.* **2003**, *1*, 347–3491